Abdillahi Bakari. 2020, 8:5
ISSN (Online): 2348-4098
ISSN (Print): 2395-4752

International Journal of Science, Engineering and Technology

An Open Access Journal

Numerical Analysis of an Un-Orthodox Stiffened Double Hull Oil Tanker Upon Impact by a Rigid Bulbous Bow

Abdillahi Bakari, Professor Emeritus Moustafa El-Gammal
Department of Naval Architecture & Marine Engineering
Tarek El Geish, El Shatby, Alexandria, Egypt,
bakariabdillahi@tum.ac.ke, mustafa.elgma@alexu.edu.eg

***Abstract*- This paper presents the design of hull structures with unorthodox light stiffeners as compared to the standard available steel sections with the aim of increasing the overall hull strength. The Y stiffeners as referred to as herein be designed, analyzed and compared to the standard Flat, L, Angle sections, Unequal angle sections and Offset bulb sections. The energy absorption capacity of the hulls strengthened by these light stiffening members and the extent of the damage on the hull plates with possible penetration and piercing of the bulbous bows are investigated. The amount of deformation on side shell plates, stringers, web frames are each studied as an indicator of the amount of distortion that can be induced as a result of the impact from the side collision. Six models of a double hull oil tanker mid-ship sections are modelled in Abaqus 6.144. They are then collided with rigid bulbous bows whose probabilistic dimensions are obtained from statistical formulas. Their results are compared to that of the Y stiffened hull. Outer hull plate rupture latest in the Y stiffened hull than all the other hulls, at a distortion of 0.2m, a total resistance force of 1518900N with a total energy dissipation of 152587J. The nearest in resistance of the other standard stiffened hulls, to the Y stiffened one are; the L and Unequal angle sections with 56% and 55% force, 45% and 44% energy of the Unequal and T3 sections to the Y hull. These results show that the Y stiffened hull possess the highest resistance to damage upon impact and the most energy absorption capacity than all the other standard stiffened hulls. The results of the FEA in Abaqus 6.144 are compared with an analytical method adopted from other researches with good agreement between the results.**

***Keywords*- Y stiffeners, Unorthodox, Deformations, Distortions, Abaqus, Energy absorption capacity.**

I. INTRODUCTION

The concept of ship collision is introduced by Minorsky in 1959 [1]. This is followed by analytical concept of collision by Zhang[2]. Liu [3] and Amdahl [3] broaden this concept into collision between structure and iceberg. Stronge, [4], developed analytically contact between two entities comparing the results with finite element simulations. Numerous studies have been performed in relation to grounding or collision accidents, including the Assessment of damage to ships [5], [6], damage prediction [7], [8], structural consequences [9], [10], hull girder collapse [11]–[13], damage scenarios[14]–[16], modelling [17]–[19] and structural designs [20], [21]. Research on grounding accidents conducted by Pedersen [22], Nguyen [23] and Hong and Amdahl [24].

In this paper, collision between a rigid bulbous bow with a deformable double hull mid-ship section from the side is simulated. The double hull ship section is modelled in Abaqus 6.144 with different light stiffening members. The longitudinals in all the

International Journal of Science, Engineering and Technology

An Open Access Journal

models vary from the standard frames of flat, offset bulb, angle sections, T sections and the innovated Y stiffeners.

The effect of each to resist damage to the hull and possible breach into the holds is evaluated. Using the same material properties for each hull structure model, same characteristics hull and bulbous bow dimensions, scantlings, location of impact, speed of striking bow the results of simulations are compared between the standard forms steel sections and the fabricated Y stiffeners.

II. MATERIALS AND METHODOLOGY

1. Brief Literature Review

Researches on impact technology in relation to scientific and virtual models [25]–[27], between 2011 until 2014, have been conducted. Wiśniewski and Kolakowski [28], explained a simplified numerical experimentation on the impact phenomenon. Numerous simulations on types of ship collisions are studied by Haris and Amdahl, [29]. Kitamura [30], proposed that, for good accuracy and pragmatism, the studies have to be based on available data, obtained from finite element analyses (numerical experiments), physical experiments, and data from real accidents, [31].

Crushing experiments of ship bow structures have been conducted as early as the 1960s. Details on these experiments have been reviewed in many references and investigated with regard to the axial crushing characteristics of the basic structural components. Progressive analysis of folding of a conical shell in addition to comprehensive axial crushing analysis are also studied, [19].

Ozguc et al., [32] suggested the application of plastic-kinematics material in creating deformable ship structure for side impact which is embraced and advanced by Bae et al., [33], applying real-life accident samples and laboratory experimentation. Extensively, Ludwik's strain hardening is well-defined and shown by Hutchinson & Neale, [34].

The ability of the structural components of the ship, that is, hull plating and frames, to resist bending, deformation, buckling, tear or failure offers merchant ships an enhanced element of safety to both the cargo and marine environment. This comes from a combination of superior mechanical properties of the material of the hull structure, proper design of the stiffening systems both the primary and secondary members and light and heavy members in addition to a sound arrangement of these framing system be it transverse or longitudinal. The ability of a designer to make an excellent choice in the type and design of stiffening system in terms of strength of the individual member and the overall hull structure is vital. This is in addition to the weight consideration of the whole structure. A good design combines weight and strength consideration to achieve optimum power and fuel economy.

2. The Innovative Y Stiffeners

Fig.1 below shows four basic standard longitudinal stiffeners that are in used for the stiffening of ships' hull plates. These are, flat, offset bulb, angle and T sections. These steel sections come in different standard sizes that can be obtained in manufacturers catalogues for references and use.

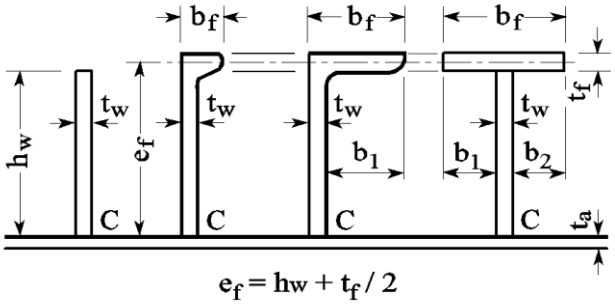

Fig.1. Standard longitudinal Stiffeners for hull plates[35].

The Y stiffener is a non-standard section built from the welding of a T section on a hat plate. The hat is made from bending or hot rolling steel plate. The hat webs are inclined at 〖45〗^° as shown in Fig. 2 below. This ensures that similar bending resistance is maintained in both the x and y axes[36]. Fig. 2 shows the nomenclature of the Y stiffeners.

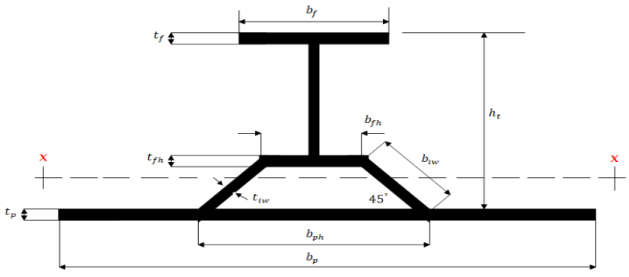

Fig. 2. Innovative Y stiffeners[36].

International Journal of Science, Engineering and Technology

An Open Access Journal

The aim of this paper is to design the Y stiffeners and compare it with equivalent standard sections during a collision analysis in terms of energy absorption, resistance to deformation, physical damage and possible hull plate breach.

3. Case Study

A double oil tanker [36], table 1, operating at the Red Sea (Gulf of Suez) having the following main particulars is chosen as the case study. The mid ship cross section of the ship is as shown in Fig. 3.

4. Design of Y Stiffeners

The design of the Y stiffeners majorly involves obtaining the section scantlings in order to be used during modelling. This is obtained by comparing the section moduli of the T stiffeners available in mid ship section in Fig. 3 with an equivalent Y section. For simplicity of analysis, only one type of T section is used in the entire hull.

Table 1. Double hull tanker main particulars.

Length Between Perpendiculars, (L_{pp})	238.0m
Moulded Depth, (D)	21.0m
Moulded Breadth, (B)	43.0m
Scantling Draught, (T)	14.3m
Deadweight, (DWT)	97,000tonnes

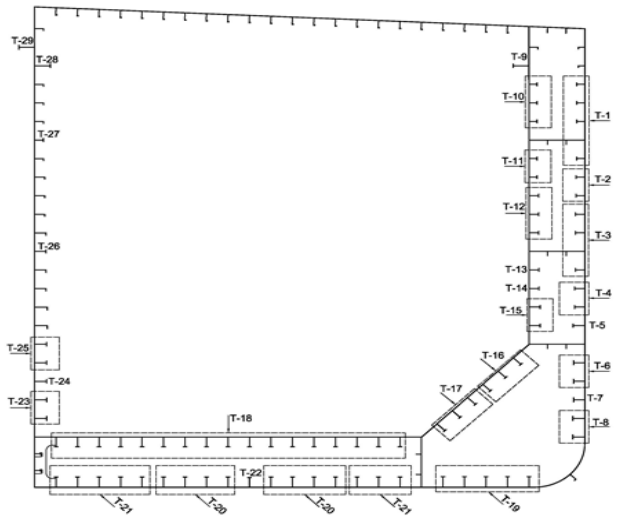

Fig. 3. Midship section of the case study double hull oil tanker with T longitudinal stiffeners in its midship section [36].

Badran [36], gave a tabulated data of Y-stiffeners compared with standard T stiffeners for the same weight or lighter weight than the T stiffeners. In addition, [36] also gave the section modulus ratio of the Y stiffener to the T stiffener. However, when comparing other standard forms such as flat, L, Unequal L and Offset bulb section to the Y stiffener, a section modulus value that will give the equivalent standard sections of the aforementioned is required. This could not be found directly from the table. As a result, calculations have to be done to find the section modulus values of the Y stiffener from the table that will allow the selection of all the other standard available sections simultaneously. The scantlings of the sections are then obtained from standard manufacturers steel section tables. In order that the double hull mid-ship section is modelled using equivalent standard stiffener to the Y stiffeners, table (2 and 3) show the Y and T stiffeners that are selected for modelling. Then from standard steel section tables of manufactures, equivalent flat, L section. Unequal L sections and offset bulb are identified and their scantlings taken for modelling six other double hull models.

Table 2. Y-stiffeners with 45° inclination angle between hat webs (with same weight as T-stiffener) [36].

	b_f	t_f	h_w	t_w	b_{fh}	t_{fh}	b_{iw}	t_{iw}
Y	285	6	682.5	3.9	69.2	9.3	101.3	9.3

h_h	b_{ph}	h_{total}	Z_{ratio}
71.65	212.5	764.8	1.452

Table 3. T-stiffeners scantlings in the midship section[36].

	b_p	t_p	A_p	h_w	t_w	A_w	b_f	t_f
Y	850	15.5	13175	350	12	4200	150	18

A_f	A_t
2700	16226

5. Equivalent Sections

In many occasions, because of the unavailability or shortage of certain profiles, equivalent sections having the same section modulus could be used. The selection of the equivalent section should satisfy, among several other requirements, the minimum weight requirement[37]. A section modulus of 936.066331 with a ratio of 3.03 (without the attached plating) in table (2 and 3) are used to obtain the equivalent flat, L, Offset bulb and Unequal L sections

International Journal of Science, Engineering and Technology

An Open Access Journal

for modelling and analysis comparisons. Based on this, the scantlings of L section[38], Unequal L section[38], Offset bulb[39] and Flat bars[40] are realized.

6. Finite Element Model (FEM)

The finite element model consists of a double hull structure and a striking bow as shown in Fig. 4 below. Modelling is done in Abaqus 6.144 CAE while the analysis is done in Abaqus Dynamic/Explicit.

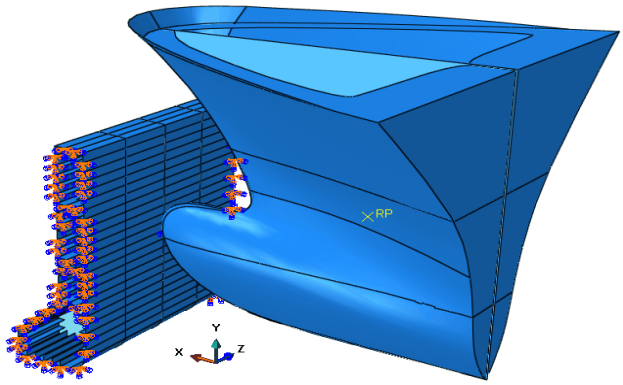

Fig. 4. Ship Side Collision Scenario of only the Double Hull Side Impacted by the Rigid Bow.

7. Selection and Modelling of the Struck ship

As previously described, the struck ship is selected from Fig. 3 with characteristic dimensions as given in table 1. Six double hull structure models of several stiffeners are modelled from 3D deformable four node shell elements with five integration points. The models are;

- Flat Stiff All
- L Stiff All
- Offset Bulb Stiff All
- T Stiff All
- Unequal Angle Sections Stiff All
- Y Stiff All

Material properties of A36 Mild Steel as shown in table 4 is used on the struck ship. A true stress strain relationship of the material can be derived from the yield stress and ultimate tensile strength [41]. By assuming the strain ϵ_y, to be 0.006 at the yield stress σ_y, [42], and the strain ϵ_ult, at the ultimate tensile strength σ_ult, is equivalent to (n)[43], the strain hardening exponent then Eqs. ((1) and (2)) can be applied. As a result, n is obtained as 0.1905 and K as 662.5 respectively, K being the strength coefficient. The finite element model is depicted in Fig. 4 above.

$$\sigma_y = K\epsilon_y{}^n = K0.006^n \quad \text{..... (1)}$$

$$\sigma_{ult} = K[ln(1+\epsilon_{ult})]^n = K[ln(1+n)]^n \quad \text{..... (2)}$$

For conformity, the same element mesh sizes are chosen for the different hull models before submitting for analysis. Ship collision analysis requires a rather coarse mesh (probably four or five elements between longitudinals, or about ten times the plate thickness) to find equilibrium between practical engineering application and reliable results [44]. For simplicity an overall plate thickness of 15.5mm for all structural components, a 100mm and 290mm mesh size for the double hull structures and rigid bows respectively are taken. This ensures that they are within the acceptable range. A fixed boundary condition encastre is selected for each to secure all the edges of the double hull, the longitudinal stiffeners, stringers and web frames. These are all defined as fixed boundary conditions. A further displacement/rotation boundary condition is applied to the tip of the rigid bow.

Table 4. A36 Steel Material Properties for the double hull[45].

Yield Stress	250MPa
Ultimate Tensile Strength	400MPa-550MPa
Mean Ultimate Tensile Strength	475MPa
Minimum Fracture Strain	0.23
Density	7800kg/m3
Young's Modulus	200GPa
Poison's Ratio	0.26

8. Selection and Modelling of the Striking Ship.

A striking ship of 70Ktons is selected. Its main dimensions (length, breadth and draught) can be obtained from graphs of statistical data. Brown [14],stated that, the relationship between the probabilistic ship principal dimensions and the ship displacement can be established for all striking ships. Similarly, the probabilistic dimensions of the bulbous bow can also be obtained using the same method of statistics.

For further simplification, the cross section of the bulbous bow is assumed to be of that of a parabola both horizontally and vertically. The tip is in addition taken as of circular cross section. This enables its dimensions to be accomplished via statistical graphs as well[46]. According to Zhang[2], the horizontal and vertical cross section of the bulbous bow could be described as a parabola. Amdahl et al[47],

International Journal of Science, Engineering and Technology

An Open Access Journal

experimented on two indenters, one with elliptical while the other with a parabolic profile. It is deduced that, a corresponding form bulbous bow would have the same mathematical calculation, hence the tip can be further idealized as a sphere. Consequently, the application of the methodology in the above literatures sources, the dimensions of the striking ship are evaluated and tabulated as in table 5 below.

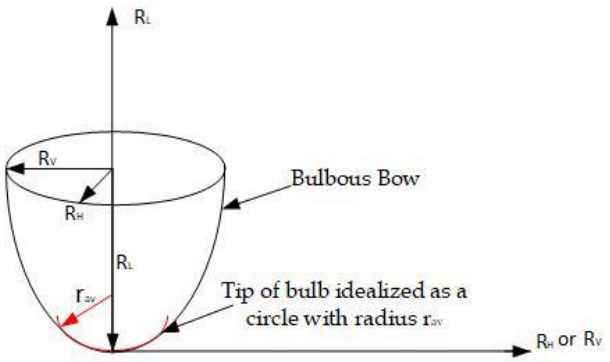

Fig. 5. (a) Determining bulbous bow shape of Striking ship and simplification of its tip.

Table 5. Striking ship dimensions.

x	$Length, L$	$Breadth, B$	$Draft, T$	R_L
70Ktons	217.39	33.11	12.35	7.39

R_H	R_V	r_v	R_h
2.98	5.24	2.69	0.87m

The striking bows are made from discrete rigid body shell-elements. A rigid reference point is defined on each of the bow form while an inertia force of 70Ktons assigned to the reference point to represent the striking ship. A coarse mesh size of 290mm is used to model the striking bow. A kinematic automatic surface to contact surface is employed with finite sliding formulation to define a penalty-based friction interaction with a coefficient of 0.3.

This is done in the dynamic explicit step in the step module. A predefined striking velocity (translation only) of 10m/s is assumed to be applied on the rigid body reference point of the striking bows within an impact time of 0.2s. The results through an evenly spaced time of 100 intervals, has been analyzed. This is to allow sufficient time to observe the plastic deformation and possible penetration of the outer plate of the hull.

II. RESULTS & DISCUSSION

1. Finite Element Results (Hulls with various Stiffeners)

The FE results of the double hull models stiffened with various standard steel sections and the innovative Y stiffeners are presented in terms of;

- Deformation patterns of shell plate, web frames, stringers, bottom transverse, and longitudinal stringers.
- Forces - Time and Force - Displacements curves.
- Response Force - Time and Response Force - Displacements curves.
- Absorbed Energies - Time and Absorbed Energies - Displacements curves.

2. Deformation Patterns

The shape of the pattern is similar for all bows due to the shape of the same bulb used to strike them. The vertical line of tear due to the tip of the bulbous bows varies in the deformation patterns they form from one hull model to the next. This depends on the amount of resistance the hull exhibits during the impact. The length and shape of the stringer and web plate portions protruding out of the material rupture line also differs from hull model to hull model. However, it is difficult to discern the extent of the resistance to the damage of the different strengthened hulls from just the outline shape of the outer hull structures from FEA, in particular when the striking bow is the same, like in this case.

Similar patterns will result. Only the inner structural members with major deformations will sow variations in deformation patterns from one hull model to another. They present the different shapes and amount of distortion at the rigid bow tip. Otherwise, the investigation of the response forces and energy absorption capacity or energy dissipation of the different structural components of the hull models can thence bring the actual difference in the strength of the various standard stiffened hull models.

In Fig. 6, the extent of distortions is maintained in the two frame and two stringer spacing. Even though the deformation pattern is the same, the amount of protrusion of the middle stringer and middle web plate is different. In a, the stringer plate more than the web plate. This length however, increases in b. In c, the amount of the web plate portion is almost equal to that of the stringer plate. In d, the web

International Journal of Science, Engineering and Technology

An Open Access Journal

frame and stringer seem to have shifted from the centre line due to the impact. Although e is similar to c, there are protrusion of either the stringer or the web plate.

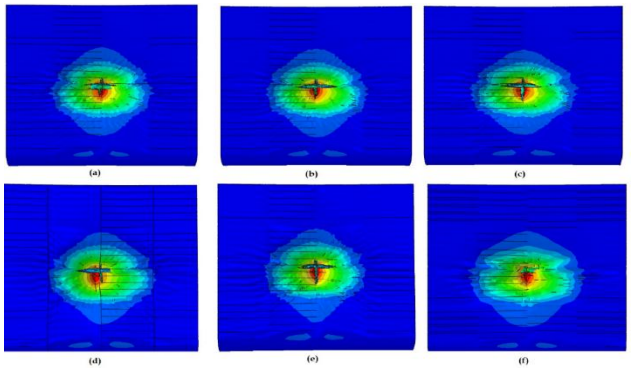

Fig. 6. Deformed hulls (a) Flat3 Stiff All (b) L3 Stiff All (c) Offset Bulb Stiff All (d) T3 Stiff All (e) Unequal L3 Stiff All (f) Y Stiff All.

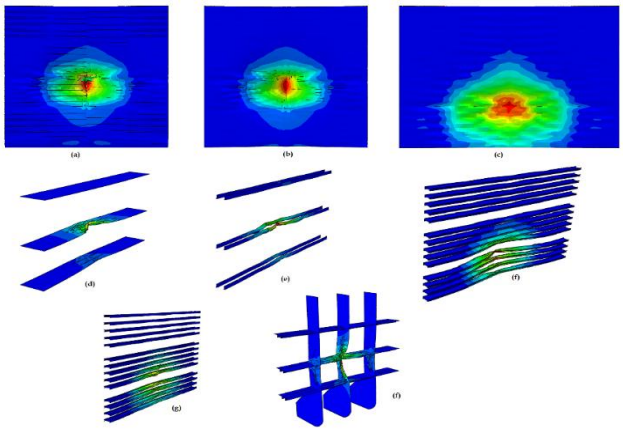

Fig.7. Y3 Stiff All Hull Model (a) Deformed hull (b) Outer Shell Plating (c) Inner Shell Plating (d) Side Stringer Plates (e) Side Stringer Longitudinals (f) Outer Hull Longitudinals (g) Inner Hull Longitudinals (h) Web frames with stringers, bilge transverse and stringer longitudinals.

3. Actual Deformations

For all the standard stiffened hull models and the Y stiffened model in the deformations in the outer hull plates (Fig.8) increase with increasing bow penetrations in the hulls. The least deformed being the L3 stiffened hull model followed by Y stiffened hull model. The offset bulb registers the most deformations among all the models. All the hull models, deform closely in a range between 1.83m to 1.88m at the end of impact period, except the L3 hull model, which reaches a peak of 1.6m. Rupture of the outer hull occur early in the Flat, L3 and Offset Bulb stiffened hull at a penetration between 0.22m to 0.24m of the bulbous bow.

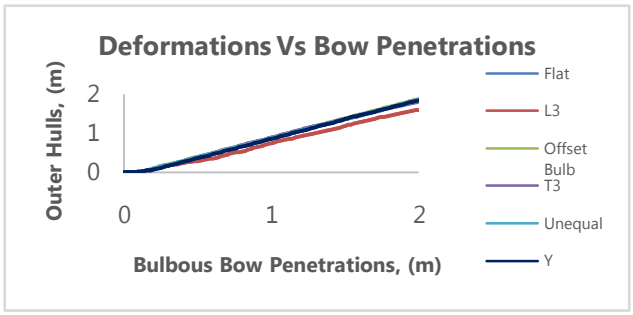

Fig.8. Graph of Deformations Vs Bulbous Bow Penetration on various stiffened outer hulls.

This is equivalent to a deformation range of 0.11m to 0.12m as shown in Fig.4.4.8. Related to the Y stiffened hull model, the T3 and the Unequal Angle sections stiffened hull models deforms at an 87% and 78% rate as compared to 59.8%, 59.1% and 52% for the L3, Offset Bulb and the flat stiffened hull models respectively. The Y stiffened hull model outer plate ruptures the last at a deformation high of 0.203m corresponding to a rigid bulbous bow indentation of 0.341m.

The outer hull longitudinals (Fig.9), shows an increasing deformation to bulbous bow penetration too. L3 and Unequal Angle stiffened hulls presents the highest increase than the others throughout the impact period. Below and beyond 1.06m of bulb penetration, the Y and Flat model OHL shows the least displacements respectively. When the onset of rupture of the outer hull begins for all the hulls, the OHL of the Y hull leads in deformation at 0.187m. This is followed by the Unequal and T3 and L3 at 0.182m, 0.177m and 0.160m respectively. This is 97, 94 and 85 percent to that of the Y model. The least deformed is that of the Flat and Offset bulb at 0.075m and 0.087m which are 40 and 46 percent compared to that of the Y model.

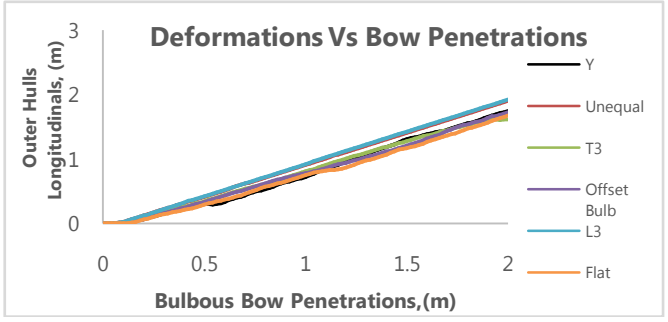

International Journal of Science, Engineering and Technology

An Open Access Journal

Fig. 9. Graph of Deformations of OH Longitudinals Vs Bulbous Bow Penetration on various stiffened hulls.

Fig. (10 and 11) shows how the stringers and stringer longitudinals deforms with subsequent rigid bow penetration respectively. The L3 and Unequal hulls records the highest plate deformations in the entire period followed by the Y model peaking at 1.74m for the two former hulls with the latter at 0.5m. However, the stringer longitudinals of the Y hull presents the highest deformations all through the entire impact period followed by the flat and T3 models. The least being the Unequal hull. At rupture of the outer plate, the closest to the Y model is the T3 model with 59.6 and 17.5 percent of stringer plate and stringer longitudinal distortions. The farthest from Y is presented by the Unequal hull model.

In Fig. 12, the web frames deformations indicate an increasing amount with bulbous bow penetrations. High ranges being presented in L3, Unequal and Flat models throughout the impact period. This varies between 1.50m to 1.57m at their peaks. Low range deformations are seen in T3, Y and Offset Bulb hulls varying between 0.35m to 0.45m. At hull plate rupture, significant deformations occur in the Unequal and Flat models with 0.14m and 0.11m respectively which are very high distortions compared to the to the Y hull model. The closest in terms of deformations are the Offset, T3 and L3 hull models with 62, 54 and 52 percent respectively.

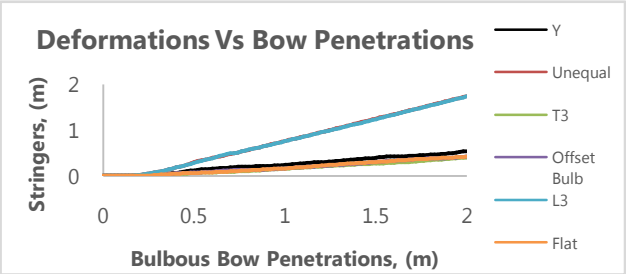

Fig. 10. Graph of Deformations of Stringers Vs Bulbous Bow Penetration on various stiffened hulls.

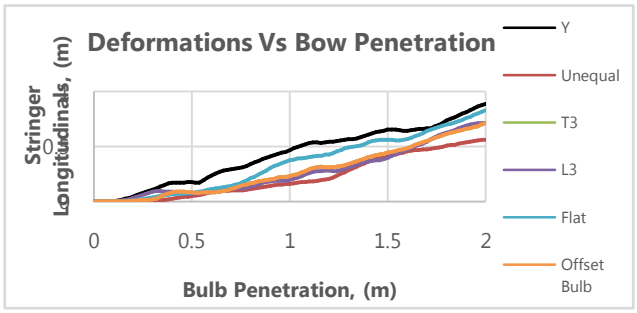

Fig.11. Graph of Deformations of Stringers Longitudinals Vs Bulbous Bow Penetration on various stiffened hulls.

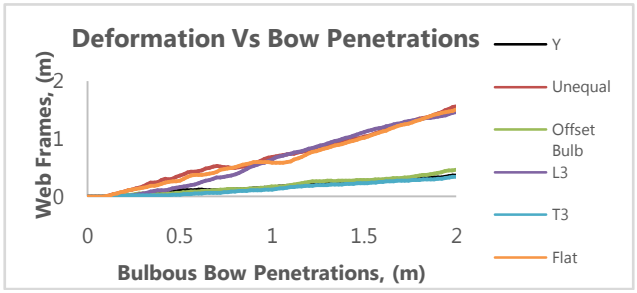

Fig. 12. Graph of Deformations of Web Frames Vs Bulbous Bow Penetration on various stiffened hulls.

Fig. (13 and 14) present the deformations of the IHL and IH with subsequent bow indentations into the hull models. The Y hull model registers the highest increment of deformations as compared with all the other stiffened models with a maximum of 0.51m and 0.53m in the IHL and IH respectively. The lowest readings being in the Offset Bulb and T3 hull models in the IHL and IH respectively. At rupture, only the Offset Bulb IHL deforms closely, at 32 percent, to that of the Y stiffened hull. The Y longitudinals displace the least. However, the inner hull of the Y model deforms the most, at 0.034m, upon rupture of the outer hull. The inner hull of the Flat model distorts the least at 0.00043m. T3 models inner hull deforms at a rate of 53 percent to that of the Y hull. The closest of all other models.

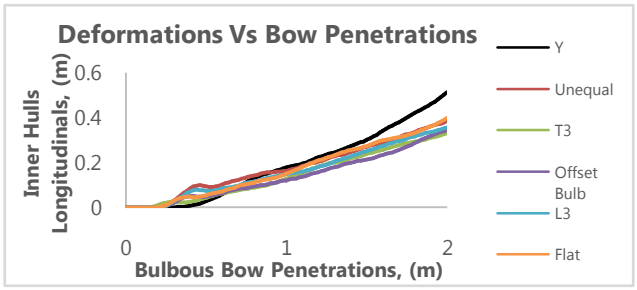

Fig.13. Graph of Deformations of Inner Hull Longitudinals Vs Bulbous Bow Penetration on various stiffened hulls.

International Journal of Science, Engineering and Technology

An Open Access Journal

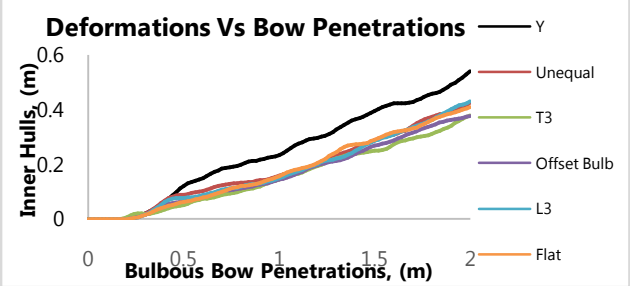

Fig.14. Graph of Deformations of Inner Hull Vs Bulbous Bow Penetration on various stiffened hulls.

Fig.15 presents a direct comparison of the deformations of the various hull components for all the different stiffened hulls. In the OH, OHL, Stringer Longitudinal and the IH, the Y stiffened components deform the most. Only the Unequal and T3 models produce deformations in the same range as that of the Y model.

Fig. 16 shows the percentage deformations of the hull components of the various strengthened hulls with respect to the Y hull. The nearest standard stiffener relating to the amount of distortion to the Y stiffeners is the T3 stiffener. This is as evidenced by the percentages to the Y sections in the various hull components studied during the analysis. The T3 hull show deformations percentages of; 87% OH, 94%OHL, 59%Stringer, 17% Stringer longitudinal, 54%Web frames and the inner hull plates.

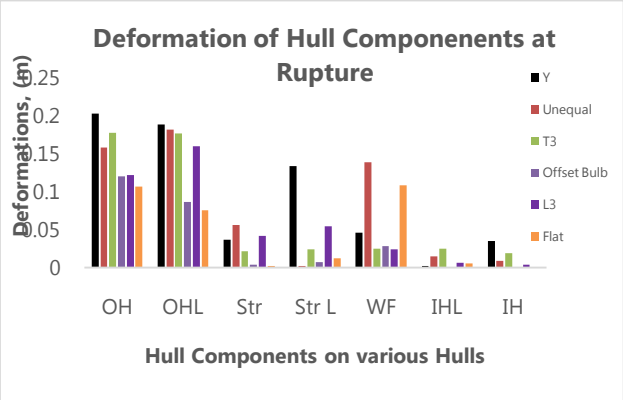

Fig. 15. Graph of Deformations of Hull Components at Outer Hull Plates Rupture on Various Stiffened Hulls.

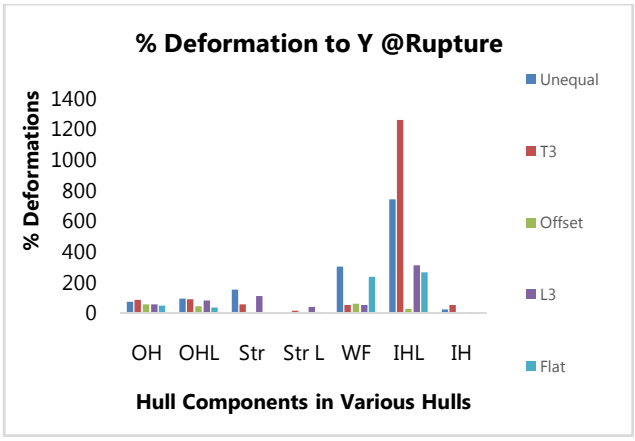

Fig. 16. Graph of %Deformations of Hull Components at Outer Hull Plates Rupture to the Y Stiffened Hull Deformation at Rupture.

In all the above description it is evident that the Y stiffeners underwent the most distortions. This is as a result of the fact that the Y stiffeners has more sectional parts than any other standard steel section due to the addition of the hat. This increases area of deformation to eventually achieve failure. As these large displacements occur, strain foci in the hull plates become less pronounced hence delay in its rupture [47]. The outer hull plates in the Y stiffened hull, ruptures later during indentation than any other hull longitudinal strengthened model.

4. Response Forces

The response in all the models is similar, with the peak of the curves indicating the point of initiation of the crack in the outer hull. Until this initial crack point of the plate is reached, the response forces keep on increasing after which they drop rapidly [46]. Fig.17 shows the response of the Y stiffened hull and the maximum point the hull material can withstand loading. Beyond this point, the hull cannot withstand any forces past its own capacity of 1518900N.

In Fig.18, the Y stiffened hull indicates the highest slope compared to all the other hull models before reaching the onset of fracture. The slope represents a corresponding measure of the amount of resistance the structure can offer before failure occurs. Failure in the Y stiffened hull occurs the latest and the highest amount of force is needed to actualize it than any other stiffened hull in the analysis, Fig. 19 and Fig. 20. L3 and Unequal angle sections strengthened hulls follow the Y hull with capacities of 853673N and 836005N respectively. This is just 56% and 55% respectively of the capacity of the Y model,

International Journal of Science, Engineering and Technology

An Open Access Journal

Fig. 21. The Flat strengthened hull presents the lowest resistance force among the entire models with a limit of 635730N. This implies that failure in this model occurs relatively earlier than all the other models.

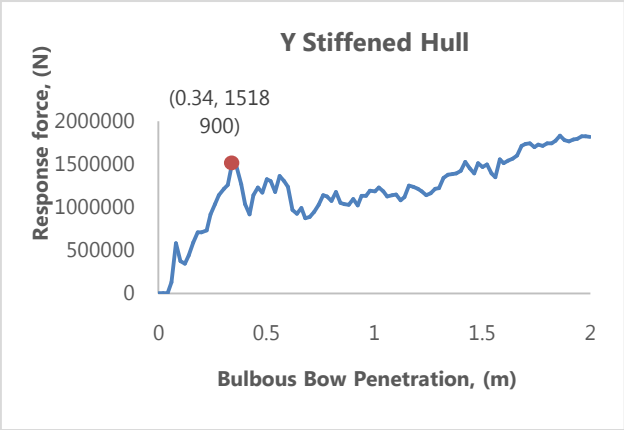

Fig.17. Graph of Response Force Vs Bulbous Bow Penetration of Y Stiffened Hull.

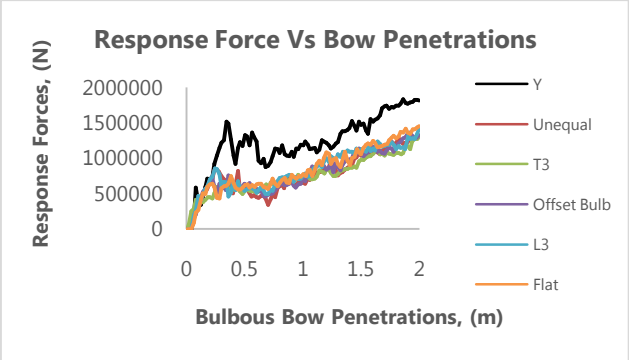

Fig.18. Graphs of Response Forces Vs Bulbous Bow Penetrations of the various Stiffened Hulls.

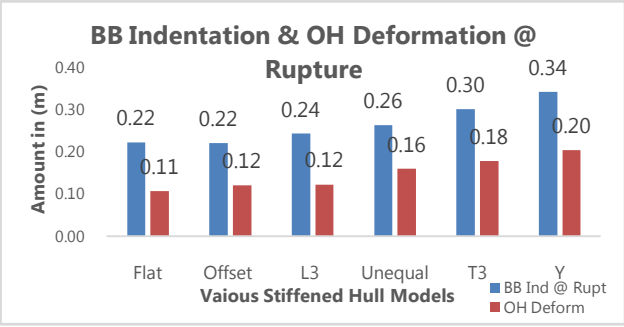

Fig. 19. Graph of Bulbous Bow Penetration and Outer Hull Deformation of the various Stiffened Hulls at rupture of the outer hulls plates.

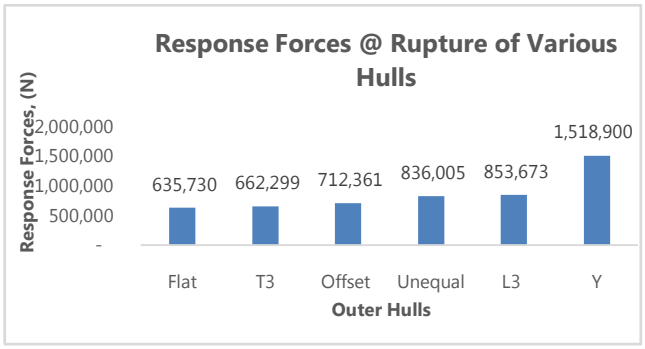

Fig.20. Graphs of Response Forces of the various Stiffened Hulls at rupture of the outer hulls plates.

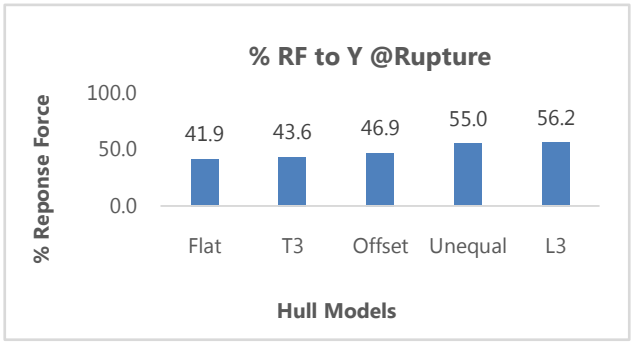

Fig.21. Graphs of %Response Forces of the various Stiffened Hulls at rupture of the outer hulls plates to the Y Stiffened Hull.

5. Absorbed Energies

Fig. 22 presents the total energy absorption capacity of all the hulls under investigation. The Y hull emerges as the one with the most energy absorption capabilities than any of the other hulls. This is then followed by the Flat and L3 hull but with a big discrepancy between them and the Y hull. At peak values, the Y hull has an energy absorption of 1512250J while the L3 and Flat model possessing 965902J and 992542 respectively of the absorbed energy. The least being that of T3 at 802721J.

In Fig.23 the Y model registers the highest increasing amount of energy absorbed during the impact period than any other model with a peak of 430392J. The other models energies are bundled within a peak range of 381703J to 395138J, T3 and Unequal models respectively. At rupture, the most absorbed energies are by the T3 strengthened model with 16895.6J followed by the Y hull with 10561.4J and the Unequal with 7057.2 J. The Flat model absorbs the least energy followed by the Offset Bulb and eventually the T3 stiffened model, compared to the Y model, the L3 and the Unequal models are the

nearest in terms of their outer hull energy absorbing capacity of 59% and 67% respectively.

5.1. Outer Hull longitudinals

Although the absorbed energies in the outer hull longitudinals is less than that of the outer hull plates, the Y stiffened hull model still presents higher values of energies compared to other models with increasing bow penetrations. It reaches its peak of 301402J while the other models cluster themselves between a range of about 96600J for the T3 and 145174J for the Flat model. At failure, OHL absorb most energy in the Y, T3 and L3 models with 22976.3J, 11092.9J and 6518.44J respectively. In this the Y model OHL absorbs twice as much energy as it takes in its OH. The least absorbed energy being that of the Unequal model with 4965.4J, Fig. 23. Among all these models, the nearest in terms of OHL energy absorption capacity to the Y hull is the T3 model with just 48%, Fig. 24.

5.2. Stringers

The Y stiffened hull still shows significant energy absorption capacity in the stringers and their longitudinals than the rest of the models. With a peak value of 176908J in the stringer plates, the other models are left within a range of 99648J and 125557J of the T3 and L3 models respectively. In the event of rupture of the outer hull plates, the Y and T3 models stringers plates absorbs the most energy of about 14143J and 8500J respectively, Fig. 23. The closest, in terms of energy absorption capacity, of the stringers to the Y model, is the T3 stiffened hull model with 60.1% rate, Fig. 24.

In the absorbed energies of the stringer longitudinals, with increasing bow penetrations, the Y stiffened hull longitudinals continues to indicate higher increasing energies than all the other models. It attains an uttermost value of 35571.6J at the end of the collision period. The other models range between peak values of 12655.4J and 15779.6J of T3 and of L3 respectively. During OH plate tear initiation, the Y hull stringer longitudinals with 867J possess the most energy as compared to the other stiffened hull models. This is twice as much as that of individual energy levels of all the other models save for the Flat model for which it is four times its energy at 222J, Fig. 23. The nearest, to the Y stiffened hull, in terms of energy absorption capacity of the stringer longitudinals is the L3 hull at just 51% that of the Y model, Fig. 24.

5.3. Web Frames

In the absorbed energy capacities for the web frames of all the stiffened hulls, the Y stiffened hull again indicates highest increasing amounts of energy absorbed in the web frames for all the strengthened hulls in investigation. It attains a peak of 436757J at the end of impact period. T3 hull model with a maximum value of 141682J and the Flat model with a maximum of 242036J forms the range between which all the remaining hulls models energies are found. During rupture of the outer hull plates, Y, Unequal and L3 models lead in energy absorption with 100029J, 52204J and 46043J respectively, Fig. 23. The nearest to the Y hull in terms of the energy absorption capacity in the web frames is the Unequal hull with just 52% rate, Fig. 24.

5.4. Inner Hull and Inner Hull Longitudinals

The energy absorption capacities of the IHL and IH of the different strengthened hulls show that with peaks of 28885J and 19761J for the IHL and IH respectively, the Y stiffened hull maintains the highest energy levels than all the other hulls stiffened by standard longitudinal sections during the entire impact period. The rest of the hull models have an absorption capacity range between that of the Flat and Unequal with 5818J to 8263J and that of T3 of 10759J to 13812J for the IHL and IH respectively. At rupture, the Y model energy absorptions are the highest at 3167J and 841J in the IHL and IH. This is followed by that of the T3 model with 496J and 591J, Fig. 23. The T3 model maintains the closest capacity in terms of energy absorption to the Y hull with a rate of 16% and 71% in the IHL and IH respectively, Fig. 24.

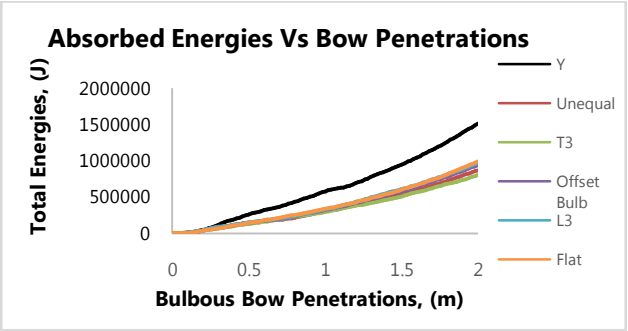

Fig. 22. Graphs of Total Absorbed Energies of Inner Hull Vs Bulbous Bow Penetrations of the various stiffened hulls.

International Journal of Science, Engineering and Technology

An Open Access Journal

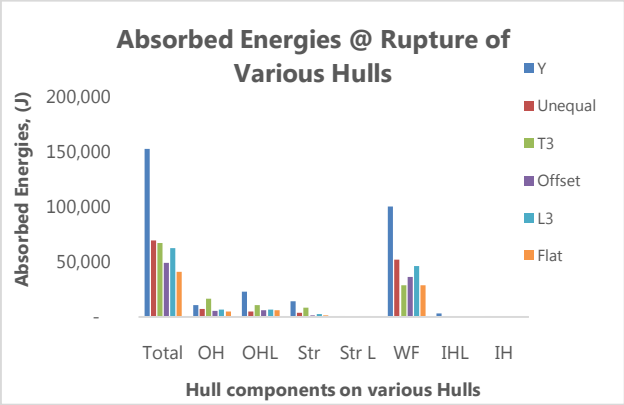

Fig.23. Graphs of Absorbed Energies of Hull Components Vs Bulbous Bow Penetrations of the various stiffened hulls at Rupture of the Outer Hulls Plates.

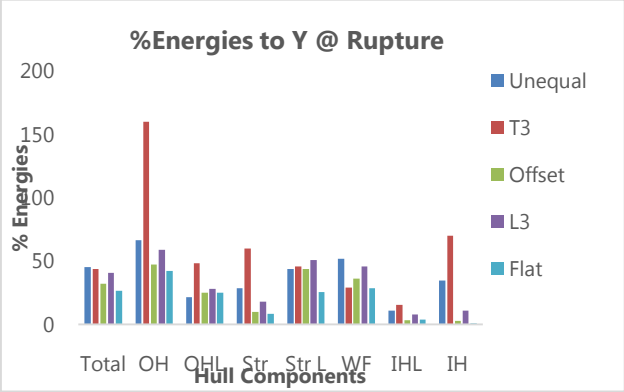

Fig.24. Graphs of %Absorbed Energies of Hull Components Vs Bulbous Bow Penetrations of the various Stiffened Hulls at Rupture of the Outer Hulls Plates.

6. Validation

Liu [46] presented a rapid method to assess the resistance of a double hull struck by a rigid bulbous bow. Using this method, the results obtained from the analytical calculations, for the Y stiffened model, for the outer hull plate only, are compared with the numerical results. The resistance force obtained at the outer shell plate is 7% more than the numerical results. The absorbed energy evaluated from integration is 9128.24J, 13.57% less than that of the numerical results of 10561.4J. The numerical results are in good agreement with the analytical formula evaluating effectively the strength of the outer hull of the Y stiffened side hull structure as shown in Fig. 25.

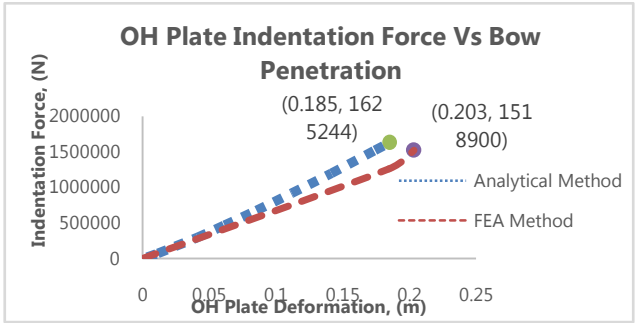

Fig. 25. Comparison between the Forces of Indentation on the outer hull plate of a Y stiffened hull by Analytical and FEA Method.

IV. CONCLUSIONS

An unorthodox new stiffener, the Y stiffener, is designed in this thesis. The designed is based on the minimum weight requirement of standard T steel sections on a double hull oil tanker case study ship. By replacing all the midship sections with equivalent sections of flat, offset bulb, L, unequal angle and the Y stiffeners, numerical analysis of the double hull models impacted by rigid bows from the side is studied.

The purpose of the study is to justify the merits of the new innovative stiffeners over the standard sections in terms of increased resistance of the hull structure to failure during impact by other ships. In order to come up with some measureable criteria to determine the crashworthiness of the various stiffened hulls, the deformations, response and energy absorption capacity of the individual hull components until fracture are investigated. A rapid analytical method is adopted from different research sources to validate the numerical results obtained. In this method, simple shape bow forms are used to come up with simple analytical formulas based on probabilistic and statistical dimensions of striking bows in relation to the striking ship's displacement to determine individual components and overall hull strength. The results from each hull are compared and the following are the deductions made:

- Except for the stringer plate and web girders, the displacements at rupture in the Y stiffened hull are the highest compared to any other standard stiffened hull in the outer shell plates, outer hull longitudinals, stringer longitudinals and the inner hull. This is due to the fact that the Y stiffeners has a bigger surface area to deform than all the other standard sections. The closest to the Y sections are

the T sections with 87%, 93%, 59%, 17%, 54% and 53% deformations in the OH, OHL, Str, Str L, WF and the IH. The least being the flat and the offset bulb stiffened hulls. Outer hull plate rupture latest in this Y stiffened hull than all the other hulls, at a bulbous bow indentation of 0.34m with a deformation of 0.2m of the plate.

- The Y stiffened hull shows the highest resistance to distortion as it has the highest response force at rupture than all the other standard stiffened hulls. The Y longitudinals increases the stiffness of the material structure the most until a capacity of 1518900N where rupture occur after a distortion of 0.2m as previously mentioned. From the onset of loading the forces increase with the deformations of the plates and stiffeners. With the Y sections having the most distortions, they resisted the highest forces until the material could withstand no more. The nearest to resistance of the other standard stiffened hulls to the Y stiffened one are the L and Unequal angle sections with 56% and 55% of the Y longitudinals resistance capacity respectively.
- The dissipated energy capacity of the Y hull is dominant to the other standard hull stiffened structures. The values in this hull indicates a towering superiority over the others throughout the entire impact period. This is proof of the enormous distortions the unique longitudinals can take as they absorbs the most energy with these displacements until fracture occur. At rupture, an enormous amount of energy of 152587J is dissipated by the entire structure with the OHL absorbing twice as much as the OH. 22976J and 10561J respectively. This is due to the twice as much displacement the OHL undergoes compared to the OH. The nearest to the Y hull in terms of the energy absorption capacity is the Unequal and T3 sections with 45% and 44% energy absorption capacity to the Y hull.
- Is evident that the Y stiffened hull exhibits superior crashworthiness properties than all the other standard stiffened hulls by an overwhelming margin as portrayed in the analysis. The Y longitudinals offer a better alternative to all the other standard steel sections giving a stronger hull against damage due to impact forces. An overall hull structure is realized when stiffened by the innovative Y stiffeners.
- The results of the FEA in Abaqus are compared with the analytical method with good agreement between the results. The OH resistance is 1625244N, 7% more than that of the numerical analysis, 1518900N. The dissipated energy obtained from the integration of the same force displacement equation is 9128.24J, 13.57% less than that of the numerical results of 10561.4J. The application of the simple method to evaluate the strength of the double hull proved effective. However, the critical distortion at rupture evaluated from the analytical method was beyond the allowable limits.

1. Nomenclature

A_f: Area of face plate
A_p: Area of attached plating
A_t: Total area
A_w: Area of web frame
b_f: Width of face plate
b_{fh}: Width of face plate of hat in Y stiffener
b_{iw}: Width of the web plate of the hat in a Y stiffener
b_p: Width of attached plate
b_{ph}: Width of the hat of a Y stiffener
h_h: Height of the hat of in a Y stiffener
h_{total} : Overall height of the Y stiffener
h_w: Depth of web plate
IH: Inner Hull
IHL: Inner Hull Longitudinal
L3: L stiffener of number three in the given table
OH: Outer Hull
OHL: Outer Hull Longitudinal
r_{av}: Average radius of the tip of the bulbous bow
r_v: Vertical radius of the tip of the bulb
R_H: Horizontal radius of the bulb
R_h: Horizontal length of the tip of the bulb
R_L: Length of Bulb
R_V: Vertical radius of the bulb
Str: Stringer
Str L: Stringer Longitudinal
T3: T stiffener of number three in the given table
t_f: Thickness of face plate
t_{fh}: Thickness of face plate of the hat in a Y stiffener
t_{iw}: Thickness of the web plate of the hat in a Y stiffener
t_p: Thickness of attached plating
t_w: Thickness of web plate
WF: Web Frame
Z_{ratio} : Section modulus ratio between stiffeners

2. Acknowledgements

This paper presents a Part of the Partial Fulfillment of the requirements leading to granting M.Sc. Degree at the Department of Naval Architecture and Marine Engineering, Faculty of Engineering, University of Alexandria, Egypt. The authors are appreciating the sponsorship of the Egyptian Government through

financial support to the First Author. The thesis is with the Supervision of the Second and Third Authors. Finally, the Technical University of Mombasa in Kenya and the Kenyan Governmental Authorities are also complemented for their support.

REFERENCES

[1] V. U. Minorsly, "An Analysis of ship Collisions with Reference to Protection of Nuclear Power Plants.pdf," Journal of Ship Research. pp. 1–4, 1959.

[2] S. Zhang, "The mechanics of ship collisions," Tech. Univ. Denmark, no. January, 1999.

[3] Z. Liu and J. Amdahl, "A new formulation of the impact mechanics of ship collisions and its application to a ship-iceberg collision," Mar. Struct., vol. 23, no. 3, pp. 360–384, 2010, doi: 10.1016/j.marstruc.2010.05.003.

[4] W. J. Stronge, "Impact Mechanics," no. November, 2000, doi: 10.1017/CBO9780511626432.

[5] G. Wang, J. Spencer, and Y. Chen, "Assessment of a ship's performance in accidents," Marine Structures, vol. 15, no. 4–5. pp. 313–333, 2002, doi: 10.1016/S0951-8339(02)00017-5.

[6] J. K. Paik, "Innovative structural designs of tankers against ship collisions and grounding: A recent state-of-the-art review," Marine Technology, vol. 40, no. 1. pp. 25–33, 2003, [Online]. Available: http://www.scopus.com/inward/record.url?eid=2-s2.0-0037252840&partnerID=tZOtx3y1.

[7] B. C. Simonsen and P. F. Hansen, "Theoretical and statistical analysis of ship grounding accidents," Journal of Offshore Mechanics and Arctic Engineering, vol. 122, no. 3. 2000, doi: 10.1115/1.1286075.

[8] B. Cerup-Simonsen, R. Törnqvist, and M. Lützen, "A simplified grounding damage prediction method and its application in modern damage stability requirements," Marine Structures, vol. 22, no. 1. pp. 62–83, 2009, doi: 10.1016/j.marstruc.2008.06.007.

[9] S. Zhang, "Plate tearing and bottom damage in ship grounding," Marine Structures, vol. 15, no. 2. pp. 101–117, 2002, doi: 10.1016/S0951-8339(01)00021-1.

[10] A. Zhang and K. Suzuki, "Dynamic FE simulations of the effect of selected parameters on grounding test results of bottom structures," Ships and Offshore Structures, vol. 1, no. 2. pp. 117–125, 2006, doi: 10.1533/saos.2006.0117.

[11] P. T. Pedersen, "Ship grounding and hull-girder strength," Marine Structures, vol. 7, no. 1. pp. 1–29, 1994, doi: 10.1016/0951-8339(94)90008-6.

[12] J. K. Paik, A. K. Thayamballi, and S. H. Yang, "Residual Strength Assessment of Ships after Collision and Grounding," Marine Technology, vol. Vol 35, no. No. 1. pp. 38--54, 1998.

[13] G. Wang, K. Arita, and D. Liu, "Behavior of a double hull in a variety of stranding or collision scenarios," Marine Structures, vol. 13, no. 3. pp. 147–187, 2000, doi: 10.1016/S0951-8339(00)00036-8.

[14] A. J. Brown, "Collision scenarios and probabilistic collision damage," Mar. Struct., vol. 15, no. 4–5, pp. 335–364, 2002, doi: 10.1016/S0951-8339(02)00007-2.

[15] M. S. Samuelides, K. Tabri, A. Incecik, and D. Demos, "Scenarios for the assessment of the collision behavior of ships," International Shipbuilding Progress, vol. 55, no. 1–2. pp. 145–162, 2008, doi: 10.3233/ISP-2008-0043.

[16] J. K. Paik, D. K. Kim, D. H. Park, H. B. Kim, and M. S. Kim, "A new method for assessing the safety of ships damaged by grounding," Transactions of the Royal Institution of Naval Architects Part A: International Journal of Maritime Engineering, vol. 154, no. PART A1. pp. 1–20, 2012, doi: 10.3940/rina.ijme.2012.al.218.

[17] K. Tabri, J. Broekhuijsen, J. Matusiak, and P. Varsta, "Analytical modelling of ship collision based on full-scale experiments," Marine Structures, vol. 22, no. 1. pp. 42–61, 2009, doi: 10.1016/j.marstruc.2008.06.002.

[18] J. K. Paik, "Practical techniques for finite element modelling to simulate structural crashworthiness in ship collisions and grounding (Part II: Verification)," Ships and Offshore Structures, vol. 2, no. 1. pp. 69–80, 2007, doi: 10.1533/saos.2006.0148.

[19] J. K. Paik, "Practical techniques for finite element modeling to simulate structural crashworthiness in ship collisions and grounding (Part I: Theory)," Ships and Offshore Structures, vol. 2, no. 1. pp. 69–80, 2007, doi: 10.1533/saos.2006.0148.

[20] J. K. Paik et al., "Collision and Grounding Final Report of ISSC V3," San Diego, USA, 2003.

[21] M. S. Samuelides, N. P. Ventikos, and I. C. Gemelos, "Survey on grounding incidents: Statistical analysis and risk assessment," Ships and Offshore Structures, vol. 4, no. 1. pp. 55–68, 2009, doi: 10.1080/17445300802371147.

[22] P. T. Pedersen, "Review and application of ship collision and grounding analysis procedures," Marine Structures, vol. 23, no. 3. pp. 241–262, 2010, doi: 10.1016/j.marstruc.2010.05.001.

[23] T. H. Nguyen, L. Garrè, J. Amdahl, and B. J. Leira, "Monitoring of ship damage condition during stranding," Marine Structures, vol. 24, no. 3. pp. 261–274, 2011, doi: 10.1016/j.marstruc.2011.02.006.

[24] L. Hong and J. Amdahl, "Rapid assessment of ship grounding over large contact surfaces," Ships Offshore Struct., vol. 7, no. 1, pp. 5–19, 2012, doi: 10.1080/17445302.2011.579003.

[25] C.-C. Liu, F.-M. Li, and W.-H. Huang, "Transient wave propagation and early short time transient responses of laminated composite cylindrical shells," Compos. Struct., vol. 93, no. 10, pp. 2587–2597, 2011, doi: 10.1016/j.compstruct.2011.04.021.

[26] Y. Zhou, "Modeling of softsphere normal collisions with characteristic of coefficient of restitution dependent on impact velocity," Theor. Appl. Mech. Lett., vol. 3, no. 2, p. 021003, 2013, doi: 10.1063/2.1302103.

[27] C. Ni, F. Jin, and T. Lu, "Penetration of sandwich plates with hybrid-cores under oblique ballistic impact," Theor. Appl. Mech. Lett., vol. 4, no. 2, p. 21001, 2014, doi: 10.1063/2.1402101.

[28] K. Wiśniewski and P. Kołakowski, "The effect of selected parameters on ship collision results by dynamic FE simulations," Finite Elements in Analysis and Design, vol. 39, no. 10. pp. 985–1006, 2003, doi: 10.1016/S0168-874X(02)00143-9.

[29] S. Haris and J. Amdahl, "Analysis of ship-ship collision damage accounting for bow and side deformation interaction," Marine Structures, vol. 32. pp. 18–48, 2013, doi: 10.1016/j.marstruc.2013.02.002.

[30] O. Kitamura, "FEM approach to the simulation of collision and grounding damage," Marine Structures, vol. 15, no. 4–5. pp. 403–428, 2002, doi: 10.1016/S0951-8339(02)00010-2.

[31] A. R. Prabowo, D. M. Bae, J. M. Sohn, A. F. Zakki, B. Cao, and Q. Wang, "Analysis of structural behavior during collision event accounting for bow and side structure interaction," Theor. Appl. Mech. Lett., vol. 7, no. 1, pp. 6–12, 2017, doi: 10.1016/j.taml.2016.12.001.

[32] O. Ozguc, P. K. Das, and N. Barltrop, "A comparative study on the structural integrity of single and double side skin bulk carriers under collision damage," Marine Structures, vol. 18, no. 7–8. pp. 511–547, 2005, doi: 10.1016/j.marstruc.2006.01.004.

[33] D. M. Bae, A. R. Prabowo, B. Cao, A. F. Zakki, and G. D. Haryadi, "Study on collision between two ships using selected parameters in collision simulation," J. Mar. Sci. Appl., vol. 15, no. 1, pp. 63–72, 2016, doi: 10.1007/s11804-016-1341-2.

[34] M. Behavior and D. Analysis, Mechanics of sheet metal forming. 1978.

[35] D. N. V Gl, "RULES FOR CLASSIFICATION Inland navigation vessels Part 3 Structures , equipment Chapter 3 Hull girder strength," no. December, 2015.

[36] S. Badran and M. Hassan, "A New Quantitative Fatigue Life Assessment using Alternative Stiffened Panels in Midship Section," no. July 2015, 2012.

[37] [37]M. Shama, Buckling of ship structures, vol. 9783642179. 2013.

[38] C. Limited, "CLIK Shipbuilding Solutions Break the Impossible," 2017.

[39] C. S. Profiles, "Bulb flats."

[40] J. S. Corporation, "STEEL SECTIONS FOR SHIPBUILDING."

[41] B. Liu, R. Villavicencio, S. Zhang, and C. Guedes Soares, "A simple criterion to evaluate the rupture of materials in ship collision simulations," Mar. Struct., vol. 54, pp. 92–111, 2017, doi: 10.1016/j.marstruc.2017.03.006.

[42] T. Sever, N.K., Choi, C., Yang, X., Altan, "Determining the flow stress curve with yield and ultimate tensile strengths, part II." Stamp. J., pp. 14–15, 2011.

[43] G. F. V. Voort, "Microindentation hardness testing In: ASM International.," no. 9, 2000, doi: 10.1017/CBO9781107415324.004.

[44] B. Liu, R. Villavicencio, S. Zhang, and C. Guedes Soares, "Assessment of external dynamics and internal mechanics in ship collisions," Ocean Eng., vol. 141, no. November, pp. 326–336, 2017, doi: 10.1016/j.oceaneng.2017.06.053.

[45] AZoM, "ASTM A36 Mild / Low Carbon Steel," pp. 1–3, 2012, [Online]. Available: http://www.azom.com/article.aspx?ArticleID=6115.

[46] B. Liu, "Analytical method to assess double-hull ship structures subjected to bulbous bow collision," Ocean Eng., vol. 142, no. September, pp. 27–38, 2017, doi: 10.1016/j.oceaneng.2017.06.062.

International Journal of Science, Engineering and Technology

An Open Access Journal

[47] S. Haris and J. Amdahl, "An analytical model to assess a ship side during a collision," Ships Offshore Struct., vol. 7, no. 4, pp. 431–448, 2012, doi: 10.1080/17445302.2011.614527.